Proceedings of the
1999 ASME Design Engineering Technical Conferences
September 12-15, 1999, Las Vegas, Nevada

DETC99/CIE-9116

SHAPE OPTIMIZATION FOR FLUID FLOW PROBLEMS USING BEZIER CURVES AND DESIGNED NUMERICAL EXPERIMENTS

Dulyachot Cholaseuk
Department of Mechanical Engineering
Columbia University, Mail code 4703
New York, New York 10027

Vijay Srinivasan
IBM Research Division
T. J. Watson Research Center
Yorktown Heights, New York 10598

Vijay Modi
Department of Mechanical Engineering
Columbia University, Mail code 4703
New York, New York 10027

Keywords : Shape Optimization, Design of Experiment, Computational Fluid Dynamics

ABSTRACT

Some problems in constrained shape optimization are considered. The goal in our optimization process is to maximize a measure of device performance computed using CAE, with a CAD compatible representation and specified geometric constraints. This approach illustrates several issues in integration of CAD and CAE systems. We test our ideas on idealized internal flow devices where the underlying device physics is governed by either the Laplace or the Navier-Stokes equations. The geometric shape of the device is represented by Bezier curves. Analysis tools such as the grid generator and the fluid flow solver are treated as a black box. The search pattern during the optimization process is suggested by the design of experiment methodology. The proposed framework is tested with one potential flow problem and two laminar flow diffuser problems.

1 INTRODUCTION

The use of computer-aided design (CAD) systems for the representation of geometry is now commonplace. Complex shapes can be defined by a few control points using NURBS or Bezier curves in order to efficiently describe, store and transmit geometry. These systems have been integrated with computer-aided manufacturing (CAM) systems to generate geometric representations of steps involved in manufacture of the part - e.g., tool paths for a CNC machine. The last three decades have also seen considerable advances in the use of computational techniques (e.g., boundary integral, finite element, finite difference, finite volume techniques) for the analysis of problems in fluid mechanics. These computational fluid dynamic techniques fall in the realm of Computer Aided Engineering (CAE) systems. The maturing of CAE systems has led to the possibility of systematic improvements in design to achieve desirable properties. When formalized this process is sometimes called “design optimization” if the performance can be characterized by an objective function and the design is systematically altered until the objective function is satisfied. Such a process now also falls within in the realm of CAE. Traditionally, analysis and design optimization or CAE of fluid flow components has been carried out without considering the advantages or limitations afforded by CAD systems. In this paper emphasis is placed on integration of the parametric representation of shape by CAD systems with computational fluid flow analysis and design optimization. The ideas are explored by examining the design of three idealized fluid flow devices. Bezier curves are used for representation of device geometry which is then optimized by means of Design of Experiments (DOE) techniques.

Earlier work in optimum design of fluid flow devices provided a reference point for the present effort. The Navier-Stokes equations are a set of nonlinear partial differential equations that are elliptic in space for steady, incompressible flow. Using ideas of variational calculus and optimal control it is possible to derive adjoint equations, the solution to which can provide the direction and magnitude in shape change that can ensure improvement in a specified objective function. A comprehensive review of such and other techniques is provided by Labrujere and Slooff (1993) and Pironneau (1984). Using the ideas of Pironneau (1974), optimum laminar flow diffusers were considered by Cabuk and Modi (1992). Similar ideas were also used in Huan and Modi (1996) for design of airfoils for minimum drag. These studies are, however, limited in the choice of objective functions, choice of boundary conditions and geometry constraints. Consequently, in spite of their computational efficiency, their applicability to practical problems is limited. Due to the highly non-linear relationship between device performance and the boundary shape, one can also possibly use derivative-free methods, treat the solver as a black box, and use a simplex search or genetic algorithm to carry out the optimization. But the high computational costs associated with each direct solution of a fluid flow problem makes such an approach impractical.

The present study seeks an algorithm that is independent of (a) the precise governing equation, (b) boundary conditions, (c) shape of the device, (d) fluid properties, and (e) geometric constraints. Towards this goal a pattern search method based on the design of experiments approach is utilized in the optimizer to determine the derivative information. These ideas have also been explored for a structural optimization problem by Zagajac (1998).

To achieve our goal, the representation of device geometry should allow the design space to be explored by as few parameters as possible in order to minimize computational effort. It would also be desirable for this representation to be compatible with CAD tools. Bezier curves provide an economic way to describe a shape. With a few control points, the shape of the curve (the idea can also be extended to 3 dimensional surfaces) can be controlled. This allows the development of an approximate mathematical model of the relationship between the objective function and the control point locations. The goal of shape optimization is to find the locations of the control points that correspond to the optimum shape. In Fig. 1, the optimizer performs optimization on the control point locations and uses the geometrical processor to convert the control point locations to the boundary points on the Bezier curves. The approach treats the flow solver as a black box. As shown in Fig. 1, inputs to the black box are the device geometry together with flow properties and boundary conditions. Output from the black box is the solution to the flow.

Section 2 gives a brief description of Bezier curves. This is followed by a short summary of design of experiments adopted for our study in Section 3. The shape optimization algorithm is described in Section 4. In Section 5 the optimization methodology is first verified using the known solution to an idealized two-dimensional channel design problem. Then the problems of the design of plane and axisymmetric two-dimensional diffusers in laminar flow are considered. These results are discussed in Section 6, and a summary is presented in Section 7.

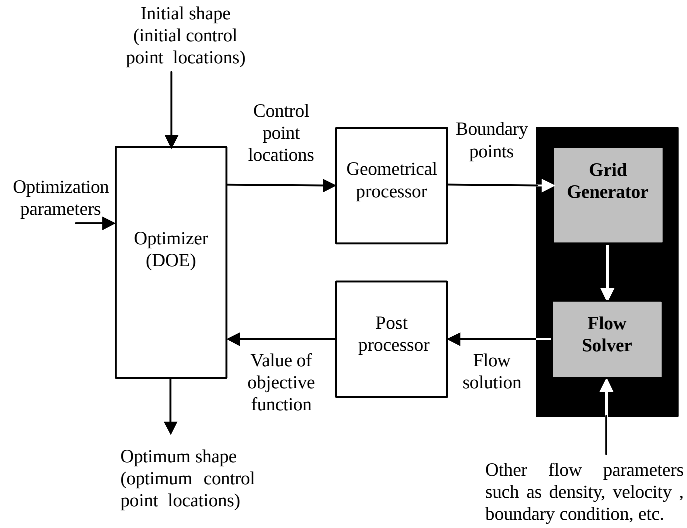

Figure 1. Overview of the optimization process.

2 BEZIER CURVE

Curves can be represented in a variety of ways. In this study Bezier curves have been chosen for the geometrical processor in Fig. 1 because of their simplicity, generality and several useful properties outlined below.

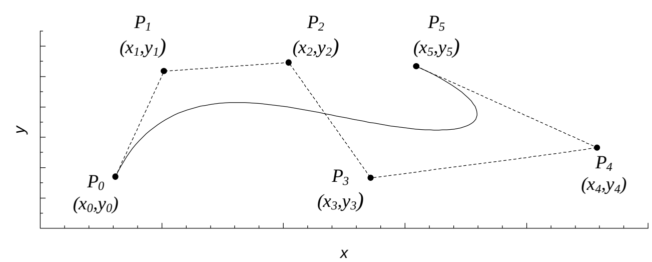

Figure 2. Bezier curve of degree 5.

Bezier curve shown in Fig. 2 is defined parametrically as

$$P(t) = \sum_{i=0}^{m} P_i\, B_{i,m}(t), \quad t \in [0,1]\,; \qquad (1)$$

where $P(t) = \begin{bmatrix} x(t) \\ y(t) \end{bmatrix}$

is point on the curve for the parametric value t,

m = degree of the Bezier curve

$P_i = \begin{bmatrix} x_i \\ y_i \end{bmatrix}$, i = 0 to m, are the control points, and

$B_{i,m}(t)$ = Bernstein basis function

$$= \frac{m!\, t^i (1-t)^{m-i}}{i!\,(m-i)!}$$

We will exploit some useful properties of Bezier curves (Farin, 1993). These are (a) Bezier curves always lie inside the convex hull of their control points, (b) Bezier curves pass through the first and last control points and the slopes of the curves on both ends equal the slopes of the corresponding control polylines, (c) a Bezier curve of degree m can be exactly represented by a new Bezier curve of degree $m+1$ by degree elevation. The first two properties are useful in handling the geometry constrains. The third property permits an increase in the degree of the curve by introducing additional control points so that the curve can represent a more complex shape when needed in the shape optimization process.

3 DESIGN OF EXPERIMENT

The optimizer in Fig. 1 relies on design of experiment, in our case a factorial analysis approach to obtain an approximate mathematical model of the system. The approach is briefly described here, with a detailed description given in Box et al. (1979).

Consider the problem of optimizing an objective function ¦$(\boldsymbol{x})$ where $\boldsymbol{x} = \{x_1, x_2, x_3, \ldots, x_n\}$. The initial value of $\boldsymbol{x}$ is identified with a super script zero as $\boldsymbol{x}^0 = \{x^0_1, x^0_2, x^0_3, \ldots, x^0_n\}$ and is called the initial point. The optimizer tries to find a new point $\boldsymbol{x}^1$ that improves the value of ¦. This is achieved by evaluating the objective function for a sample of data points in the neighborhood of the initial point. This sample is selected on the vertices of a hypercube, which is known as a full factorial analysis. The objective function values obtained at these sample data points can be used to construct a multi-linear response surface.

The size of the neighborhood is specified by the ranges of x_i, denoted as $\pm Dx_i$. These ranges are then used to obtain the normalized points $\boldsymbol{X}^0$ such that $X^0_i = 0$, the normalized ranges $\pm DX_i = \pm 1$, and the objective function $F(\boldsymbol{X})=$ ¦$(\boldsymbol{x})$. For n=2, Fig. 3 shows a graphical representation of the $2^n + 1$ data points on which the experiments were conducted (each experiment involves one direct solution). The data points consist of one initial point (open circle in Fig. 3) and its 2^n neighbors (solid circles in Fig. 3) at the vertices of a square (or cube for $n=3$, hypercube for $n > 3$).

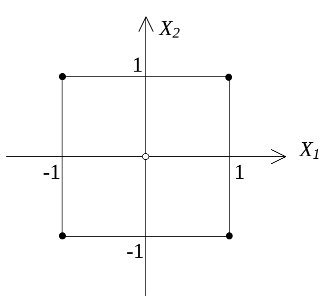

Figure 3. Graphical representation of the data points for *n*=2.

Once the objective function is evaluated at all the data points in Fig.3, we can build an approximate mathematical model from this data. For small Dx_i, $F(\boldsymbol{X})$, an estimate of the objective function $F(\boldsymbol{X})$, can be approximated as a multi-linear function

$$F(X_1, X_2, X_3, \ldots X_n) = C_0 + C_1X_1 + C_2X_2 + C_3X_3 + \ldots + C_nX_n + C_{n+1}X_1X_2 + C_{n+2}X_1X_3 + C_{n+3}X_2X_3 + \ldots + \ldots + C_kX_1X_2X_3\ldots X_n, \text{ where } k=2^n-1 \tag{2}$$

Using Yate's algorithm (described in Box et al., 1979), we can easily solve for the coefficients C_i to build the model in Eq. (2). Once the model is built a steepest direction vector, $\boldsymbol{v}$ is obtained from $v_i = dF/dX_i$ at the point $\boldsymbol{X}^0$ and is given by $\boldsymbol{v} = \{C_1, C_2, C_3, \ldots, C_n\}$. Upon normalizing the vector $\boldsymbol{v}$, a unit steepest direction vector $\boldsymbol{V}$ is obtained. Since the model is valid only around the point $\boldsymbol{X}^0$, a tentative new point $\boldsymbol{X}'$ is obtained by moving a small distance $d*R$ where R is a radius of the search which is $sqrt(n)$ and d is approximately 1. This new point is given by

$$\boldsymbol{X}' = \boldsymbol{X}^0 \pm d*R*\boldsymbol{V} \tag{3}$$

(Add $d*R$ for maximization and subtract $d*R$ for minimization)

The tentative point $\boldsymbol{X}'$ is not yet the point $\boldsymbol{X}^1$ for the next iteration. Assume that the optimization problem is that of maximizing the objective function. In order to determine the new point we must consider the following three cases:

Case 1. $F(\boldsymbol{X}')$ is greater than the maximum of the objective function at the 2^n+1 data points of Fig. 3. Then the search continues along the steepest direction until there is no further improvement of the objective function. The next iteration begins at this point.

Case 2. The maximum occurs at a vertex of the hypercube. Then that vertex is chosen as the origin for the next iteration.

Case 3. The maximum occurs at the initial point. Then a smaller hypercube of half its original size is constructed and the whole process is repeated until the size of the hypercube is smaller than some critical value.

The search pattern for maximizing $F(\boldsymbol{X})$ during one such iteration process for $n=2$ is shown in Fig. 4 where the first and the third iterations correspond to case 1, the second iteration to case 2 and the fourth, fifth and the sixth iterations to case 3.

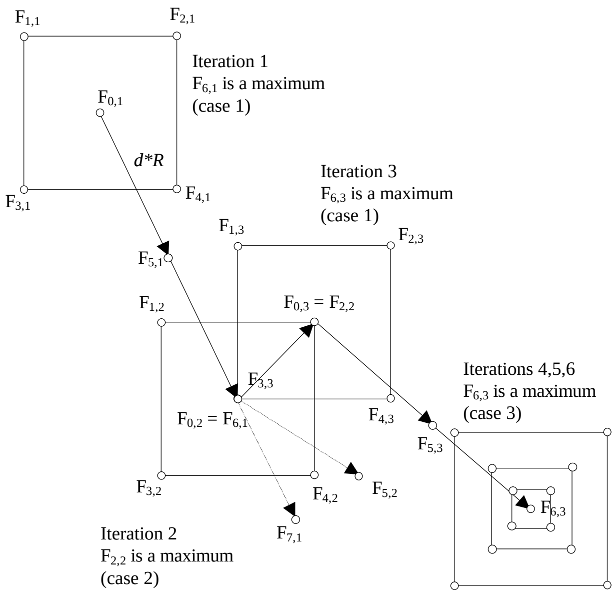

Figure 4. Search pattern for maximizing $F(X_1,X_2)$.

4 ALGORITHM FOR SHAPE OPTIMIZATION

This section describes the steps of the optimization algorithm.

Step 1. Represent the initial boundary of interest with a degree *m* Bezier curve. The initial optimization parameters are also specified at this step. These are: the initial hypercube size, the smallest critical size of the hypercube, the maximum number of iterations and the maximum number of control points. Value of an objective function, ¦, depends on the locations of the control points.

$$\begin{aligned} \text{¦} &= \text{¦}(P_0, P_1, \ldots, P_m) \\ &= \text{¦}(x_0, y_0, x_1, y_1, \ldots, x_m, y_m) \end{aligned} \quad (4)$$

Step 2. Apply geometrical constraints to the control points. These constraints may consist of
a) fixing the end point of the curve
b) fixing either *x*- or *y*-coordinates of all the control points
c) fixing the slope at one of the end points of the curve.
When this is done, the $2m+2$ variables in Eq. (4) are reduced. The remaining coordinates are considered to be the *n* variables for Eq. (2).

Step 3. Use the design of experiment procedure described in the previous section to find the new point given by the values of the *n* variables in order to improve the objective function. The new values of the *n* variables at each iteration define the new locations of the control points. These control points describe the new shape of the curve and hence the boundary points on the new curve. Note that the black-box solver (consisting of the grid generator and the flow solver) is used to compute the values of the objective function for any given set of boundary points on the curve. Each implementation of step 3 is considered one design iteration. Note that one design iteration consists of several direct solutions.

Step 4. Check whether the following criterions are satisfied.
a) the size of the hypercube is smaller than prescribed smallest critical size
b) there is no improvement in the objective function for two consecutive iterations
c) the prescribed maximum number of iterations has been reached.
If none of these conditions is met then return to step 3. If any of these conditions is met, then go to step 5.

Step 5. Check if any of the following two conditions is met:
a) There has been no improvement in the objective function between the current degree of the Bezier curve and the lower degree curve.
b) The prescribed maximum degree of the Bezier curve is reached.

If either of these conditions is met then stop the entire optimization process. If not, then increase the degree of the Bezier curve by one through degree elevation and repeat the optimization process by returning to step 2.

5 EXAMPLE PROBLEMS

5.1 Potential flow through a channel

An idealized problem with an obvious optimum shape for a given objective function is selected for validation first. The flow is assumed to be inviscid with a vorticity free inlet velocity profile. Hence the fluid flow reduces to potential flow, which in two dimensions permits the use of a simplified governing equation given by the Laplace equation. The flow within a two-dimensional channel bounded by two slip walls is considered as shown in Fig. 5. The geometric constraints are prescribed inlet width, outlet width, and a prescribed straight lower wall. The flow through the channel is given by $\nabla^2 y = 0$, where y is the stream function. The *x*- and *y*-components of the velocity are $u = -dy/dy$ are $v = dy/dx$ respectively. An additional constraint in the boundary conditions is now imposed. The flow at inlet and outlet is prescribed to be plug flow (u=1) so that $y = -y$ at $x = 0$ and 1. The objective function is specified to be the average of the absolute values of the *y*-velocity component over the inlet and the outlet or V = average$\{|(dy/dx)|_{inlet\&outlet}\}$. The optimization problem is then the determination of the upper wall shape in order to minimize V. This problem has an obvious solution given by a straight upper wall between the inlet and the outlet.

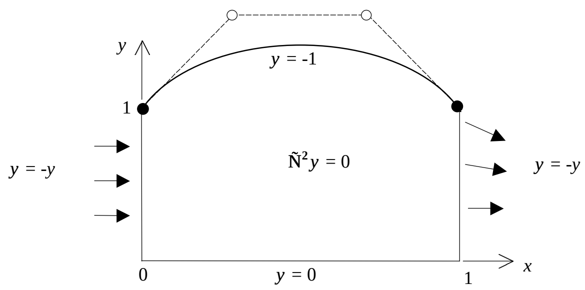

Figure 5. Potential flow through a channel.

For this particular problem a fixed number of control points - 4 control points (degree 3-Bezier curve) - were used to describe the upper wall. Hence in this problem the step 5 of section 4 is not relevant. Because of the geometry constraints of fixed inlet and outlet widths this reduces the number of variables to 4, i.e. the *x* and *y*-coordinates of the two interior control points. In addition the *x*-coordinates of the interior control points were also kept fixed reducing the number of variables *n* to 2. Boundary integral equation method (BIEM) by Liggett and Lui (1983) was used to solve the problem. The use of BIEM reduces the solution of the Laplace equation to a set of linear algebraic equations defined only on the domain boundary.

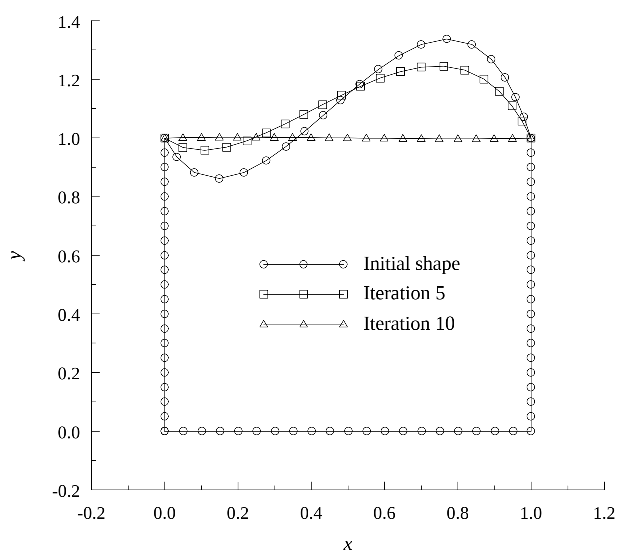

Figure 6. Result from the optimization algorithm.

An initial shape that was far from the optimum was selected to begin the optimization process. The wall to be optimized, the fixed lower wall, the inlet and the outlet were each divided into 20 segments resulting in a total of 80 grid points. This number was determined to be adequate from a grid convergence study. The initial shape as well as the shape of the wall after 5 and 10 iterations is shown in Fig. 6. The value of the objective function for the initial shape was *V*= 0.235. After 5 and 10 iterations *V* reduced to 0.099 and 0.011 respectively. The shape after 10 iterations is observed to be nearly a straight line. The entire optimization process required approximately 60 direct solutions.

5.2 Plane symmetric diffuser in laminar flow

The second problem examined was that of determining the shape of a plane symmetric diffuser that leads to the maximum pressure rise under certain flow, boundary and geometry constraints. The flow is assumed to be steady, laminar incompressible flow governed by the Navier-Stokes equations. Note that unlike the problem in section 5.1, the flow is no longer a potential flow and cannot be treated by a BIEM method. Due to symmetry, only the symmetric half of the diffuser is considered and is shown in Fig. 7. The diffuser centerline has symmetry boundary conditions and the upper wall is a no-slip wall. A parabolic velocity profile corresponding to a fully developed laminar channel flow is specified at the inlet. The geometry constraints are: prescribed inlet width *H*, prescribed diffuser length *3H*, constant length inlet and outlet sections of size *0.75H* and *6H* respectively. The objective is to maximize the pressure rise though diffuser. The pressure rise also depends upon the flow rate through the diffuser, characterized by the non-dimensional parameter, Reynolds number $Re = u_iH/n$ where n is the kinematic viscosity of the fluid and u_i is the average inlet velocity. A non-dimensional pressure rise is defined by a pressure coefficient C_p given as,

$$C_p = \frac{p_o - p_i}{\frac{1}{2} r \, u_i^2} \tag{5}$$

where p_o and p_i are the area averaged diffuser outlet and inlet pressures and r is the fluid density.

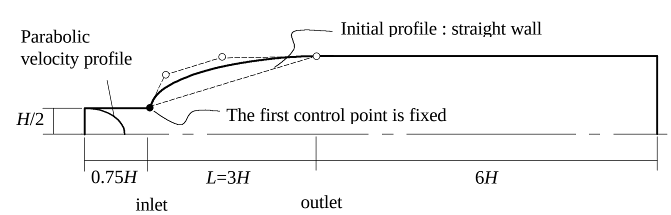

Figure 7. Plane symmetric diffuser.

The initial diffuser shape was represented by a Bezier curve with the first control point always kept fixed at the inlet and the *x*-coordinate of the others kept fixed during the optimization process. The actual control points were successively increased as described in Section 4 beginning with 3 points up to a maximum of 6 control points. A laminar fluid flow code, CAFFA by Ferziger and Peric (1996), was modified for use as the flow solver.

Figure 8 shows a typical grid of 55×10 that was used for the computation. The CAFFA flow code is a multi-grid flow solver that automatically generates a second finer grid of twice the density in each direction, i.e. 110×20 by interpolating the original 55×10 grid.

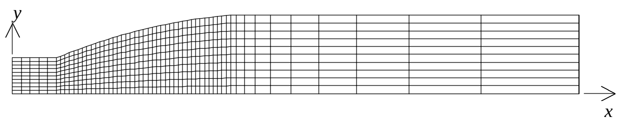

Figure 8. Typical grid of 55x10.

Because of the inherent inability of any flow solver to accurately predict the pressure coefficient with more that two significant figures, the optimization process was terminated when the second significant figure in C_p was no longer altered, although three significant figures were used in computing the steepest direction. The choice of the initial diffuser profile is made in the following fashion. The pressure coefficient for a given Reynolds number is computed for a progressively increasing diffuser area ratio *AR* (exit width/inlet width) for straight walled diffusers. The pressure coefficient achieves a maximum at some value of *AR* during this process. The straight wall profile corresponding to this area ratio *AR* is assumed to be the initial diffuser profile for a given Reynolds number. The improvement in C_p over the C_p value for a straight walled diffuser represents the gain in pressure rise due to shaping of the diffuser with a Bezier curve.

Diffuser shape optimization using ideas described in Section 4 is carried out for *Re* = 50, 100, 200 and 400. The optimized diffuser shapes are shown in Fig. 9. Note that only the diffusing portion of the upper wall is shown in Fig. 9. The constant width inlet and exit sections are not shown. The case for *Re*=100 is discussed in further detail. The optimum shape obtained in the present study is compared in Fig. 10 to the results of Cabuk and Modi (1992) obtained using an adjoint variable method derived using ideas of Pironneau (1974). The close agreement in diffuser profiles obtained with these two different optimization techniques and two different flow solvers, lends a degree of confidence to the present computations.

A plot of C_p versus *AR* for all the direct solutions is shown in Fig. 11 in order to describe the optimization process for this particular case. The solid curve represents the straight walled diffusers computed in order to select an initial shape. Each direct solution is shown on the plot as a single point. The dotted lines connect the points corresponding to the optimum shapes obtained at the end of each iteration. The C_p value for the optimum shape is 0.45 as compared to 0.41 for the initial shape. Observe that the optimum diffuser profile at *Re*=100 has a lower area ratio than the best straight walled diffuser and yet produced a larger pressure rise. This is found to be true for all the Reynolds numbers that were examined.

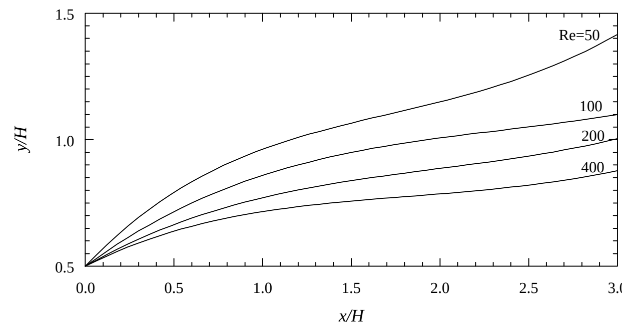

Figure 9. Optimum plane diffuser profiles with *L/H*=3 at *Re*=50, 100, 200 and 400.

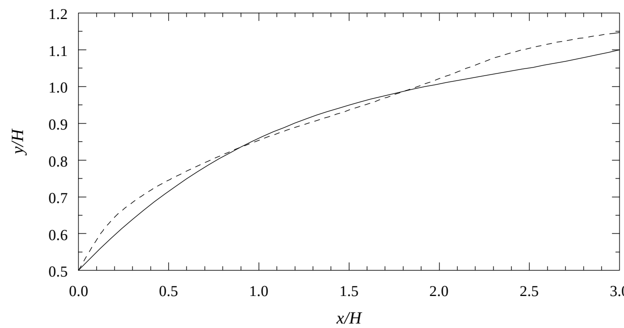

Figure 10. Optimum plane diffuser profiles with *L/H*=3 at *Re* =100. The dashed line is the result from Cabuk and Modi (1992) for a grid of 31x11 and the solid line is the present result.

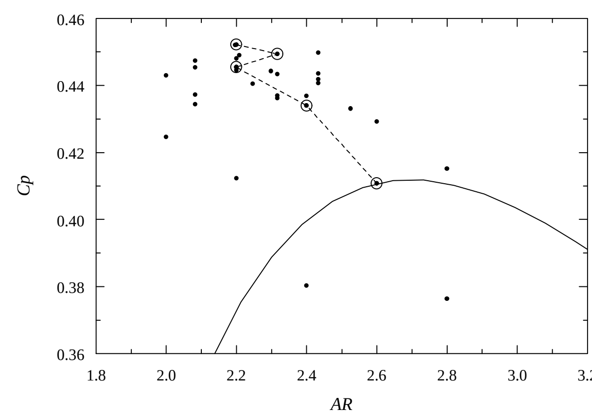

Figure 11. Pressure coefficient vs area ratio for plane symmetric diffusers with *L/H*=3 at *Re* =100.

5.3 Axisymmetric diffuser in laminar flow

The problem of optimizing axisymmetric diffusers in laminar flow is addressed next. The diffuser configuration, flow assumptions, boundary conditions and the geometry constraints are identical to those considered in section 5.2 except that now axisymmetric diffusers with inlet diameter *D* (replacing inlet width *H*) are used instead of plane diffusers. Once again optimum diffusers for laminar flow Reynolds numbers of 50, 100, 200 and 400 are computed. The final results of the optimization process are shown in the Fig. 12. Figure 13 shows the convergence of C_p during the optimization process for the case of *Re*=100.

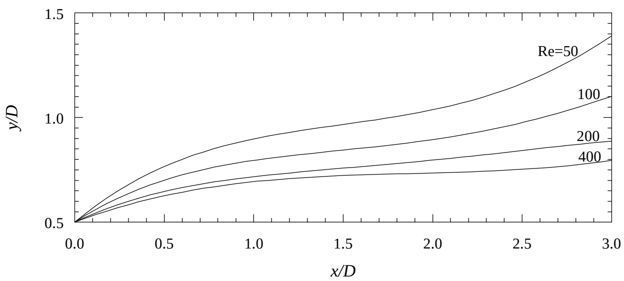

Figure 12. Optimum axisymmetric diffuser profiles with *L/D*=3 at *Re* = 50, 100, 200 and 400.

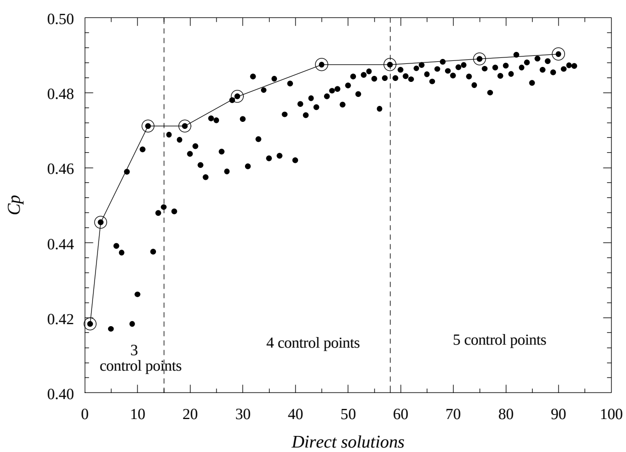

Figure 13. The progression of the pressure coefficient with each direct solution during the optimization process of axisymmetric diffusers with *L/D*=3 at *Re*=100. Each point represents a single direct solution. The solid line segments connect the optimum results after each design iteration.

6 DISCUSSION

For the potential flow problem of section 5.1 we verified that the algorithm was able to achieve the optimum shape by changing as few as two control points. In section 5.2 and 5.3 we applied the algorithm to two laminar diffuser problems and the results were also encouraging. Significant improvement in C_p's for both plane and axisymmetric cases is achieved for all the Reynolds numbers in the study.

Consider the result of the optimization process for the plane symmetric diffuser at *Re*=100. The maximum C_p obtained from computations is 0.452. Since we expect no more than a two significant figure accuracy from the solver, CAFFA, we consider the maximum to be C_p=0.45 and the intermediate results with C_p>0.445 obtained during the optimization process to correspond to optimum profiles. With this in mind, the optimum region lies above C_p=0.445 as shown in Fig. 14. This implies that there is a family of profiles obtained from the optimization process that can be considered optimum. These profiles are shown in Fig. 15 corresponding to the points in optimum region of Fig. 14.

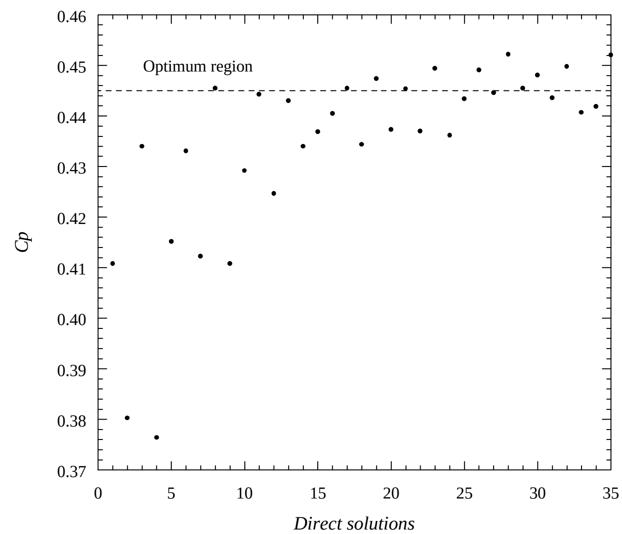

Figure 14. The progression of pressure coefficient with each direct solution during the optimization process of plane diffusers with *L/H* = 3 at *Re*=100.

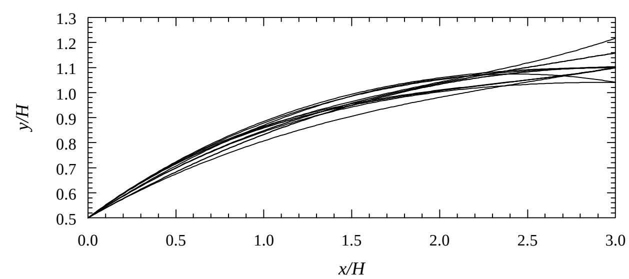

Figure 15. Family of optimum plane diffuser profiles with *L/H*=3 and *Re*=100

7 SUMMARY

Constrained shape optimization problems for the design of fluid mechanical devices are solved. These problems highlight some of the issues that arise in the integration of CAD with CAE. Bezier curves were utilized to represent device shapes and to incorporate geometric constraints.

Bezier curves lend themselves to an adaptive increase in their degree as needed leading to a richer design space as suggested by the optimization algorithm. This advantage was exploited in the optimization program that was developed and successfully tested. A full factorial design of experiment analysis requires 2^n direct solutions which can become unacceptably large as the number of degrees of freedom n increases. This is particularly true of fluid mechanics problems where CAE tools are prohibitively CPU intensive because of the coupled nonlinear PDE's used to describe the flow physics. To make the problem computationally tractable it is imperative that the number of degrees of freedom is as small as possible. This was achieved by exploiting the property that Bezier curves can describe a rich design space with a few control points. The examples we have studied involved up to 100 direct solutions and all computations were carried out on a PC.

Future work will be directed towards better geometric representation of device shapes using NURBS and improved optimization schemes. The search pattern used in our optimization algorithms allows us to study the neighborhood around any design point quite thoroughly. Future work will also explore how this information can lead to a more rational approach to robust design.

ACKNOWLEDGMENTS

The authors are grateful to Prof. Dr. Milovan Peric of Hamburg University for providing us with the CAFFA flow code.

REFERENCES

Box, G. E. P., W. G. Hunter and J. S. Hunter, 1979, “Statistics for Experiments” 2nd edition, Longman, London.

Cabuk, H. and V. Modi, 1992, “Optimum Plane Diffusers in Laminar Flow”, Journal of Fluid Mechanics, Vol 237, pp. 373-393.

Farin G., 1993, “Curves and surfaces for computer aided geometric design: a practical guide” 3rd Edition, Academic Press, Inc.

Ferziger, J. H. and M. Peric, 1996 “Computational Methods For Fluid Dynamics”, Springer-Verlag.

Huan, J. and V. Modi, 1996, “Design of Minimum Drag Bodies in Incompressible Laminar Flow”, Inverse Problem in Engineering, Vol. 3, pp. 233-260.

Labrujere, Th. E., and Slooff J. W., 1993, “Computational Methods for the Aerodynamic Design of Aircraft Components”, Ann. Rev. of Fluid Mech., Vol. 25, pp. 183-214.

Liggett, J. A. and P. L.-F Lui, 1983, “The Boundary Integral Method for Porous Media Flow”, George Allen & Unwin Ltd., London.

Pironneau, O., 1974, “On Optimum Design in Fluid Mechanics”, Journal of Fluid Mechanics, Vol. 64, pp. 97-110.

Pironneau, O., 1984, “Optimal Shape Design for Elliptic Systems”, Springer-Verlag.

Zagajac, J., 1998, “Constrained shape optimization: Can geometric modeling and engineering analysis system cooperate?”, presented at the SIAM workshop on Mathematical Foundation for Feature in Computer-Aided Design Engineering and Manufacturing, October 1998, Troy, Michigan.

